Nonlinear Analysis of Anisotropic Panels

Ahmed K. Noor* and Jeanne M. Peters†
George Washington University Center, NASA Langley Research Center, Hampton, Virginia

A computational procedure is presented for the efficient nonlinear analysis of symmetric anisotropic panels. The three key elements of the procedure are: 1) use of three-field mixed models having independent interpolation (shape) functions for stress resultants, strain components, and generalized displacements, with the stress resultants and strain components allowed to be discontinuous at interelement boundaries; 2) decomposition of the material stiffness matrix into the sum of an orthotropic and a nonorthotropic (anisotropic) part; and 3) successive application of the finite element method and the classical Rayleigh-Ritz technique. The finite element method is first used to generate a few global approximation vectors (or modes). Then the amplitudes of these modes are computed by using the Rayleigh-Ritz technique. The global approximation vectors are taken to be various-order derivatives of the strain components, stress resultants, and generalized displacements with respect to an anisotropic tracing parameter and a load parameter; they are evaluated at zero values of the two parameters. The size of the analysis model used in generating the global approximation vectors is identical to that of the corresponding orthotropic structure. The effectiveness of the proposed computational procedure is demonstrated by means of a numerical example, and its potential for solving quasi-symmetric nonlinear problems of composite structures is discussed.

Nomenclature

E_L, E_T = elastic moduli of the individual layers in the direction of fibers and normal to it, respectively
$F_{\mathcal{J}\mathcal{J}}$ = linear flexibility coefficients of the shell element
G_{LT}, G_{TT} = shear moduli in plane of fibers and normal to it, respectively
$H_{\mathcal{J}}$ = stress resultant parameters
h = thickness of the shell
$\mathfrak{K}_{\mathcal{J}\mathcal{J}}, \mathcal{K}_{\mathcal{J}\mathcal{J}}$ = orthotropic and nonorthotropic parts of the $K_{\mathcal{J}\mathcal{J}}$ array, see Eqs. (1)
$\tilde{\mathfrak{k}}_{ij}, \tilde{\mathcal{k}}_{ij}$ = orthotropic and nonorthotropic parts of the linear stiffness coefficients of the reduced system, see Eqs. (7-9)
$k_{\alpha\beta}$ = curvatures and twist of the middle surface of the shell
L_1, L_2 = side lengths of the panel
$M_{\alpha\beta}$ = bending stress resultants
$\mathfrak{M}_{\mathcal{J}JL}$ = nonlinear element coefficients, see Eqs. (2) and (3)
$\tilde{\mathfrak{m}}_{ijk}$ = nonlinear coefficients of the reduced system, see Eqs. (7) and (10)
m = number of displacement nodes in the element
$N_{\alpha\beta}$ = extensional (in-plane) stress resultants
p_0 = intensity of uniform transverse loading
Q_α = transverse shear stress resultants
Q_I = normalized external load components, see Eqs. (3)
$\tilde{\mathcal{Q}}_i$ = load components of the reduced system, see Eqs. (11)
q = load parameter
R = radius of curvature of the shell middle surface
r = number of global approximation vectors
$R_{\mathcal{J}\mathcal{J}}, S_{\mathcal{J}J}$ = generalized stiffness coefficients of the shell element, see Eqs. (1-3)
$\mathcal{o}$ = number of parameters used in approximating each of the stress resultants and strain components
U = total strain energy of the shell
U_0 = strain energy corresponding to $\lambda = 0$
u_α, w = displacement components in the coordinate directions
X_I = nodal displacement parameters
x_α, x_3 = orthogonal curvilinear coordinate system
$\epsilon_{\alpha\beta}$ = extensional strains of the shell middle surface
$2\epsilon_{\alpha 3}$ = transverse shear strains of the shell
$\kappa_{\alpha\beta}$ = curvature changes and twist of the shell middle surface
$\bar{\beta}$ = condition number of the Gram matrix of the basis vectors
$\Gamma^{(\Phi)}_{\mathcal{J}i}, \Gamma^{(H)}_{\mathcal{J}i}, \Gamma^{(X)}_{Ii}$ = matrices of global approximation vectors defined in Eqs. (4-6)
ν_{LT} = major Poisson's ratio of the individual layers
$\Phi_{\mathcal{J}}$ = strain parameters
λ = parameter identifying all the nonorthotropic (anisotropic) contributions in the stiffness arrays
ϕ_α = rotation components
ρ_ℓ = parameters measuring the sensitivity of the global response of the structure to nonorthotropic material coefficients, see Eq. (16)
ψ_i = unknowns of the reduced equations (amplitudes of global approximation vectors)

Superscripts

t = transposition
$\dot{(\ )}$ $\equiv \frac{\partial}{\partial q}(\ )$
$(\ )'$ $\equiv \frac{\partial}{\partial \lambda}(\ )$

Range of Indices

Uppercase Latin = 1-5 m
Uppercase script = 1-8 $\mathcal{o}$
Lowercase Latin = 1-r
Greek = 1,2

Introduction

ALTHOUGH considerable literature has been devoted to the analysis of isotropic and orthotropic panels, investigations of the nonlinear and postbuckling responses of anisotropic panels are rather limited in extent. Interest in the use of filament-winding techniques for manufacturing composite

Received Aug. 27, 1985; revision received Jan. 6, 1986.

*Professor of Engineering and Applied Science.
†Programmer Analyst.

panels has recently been expanded in aircraft, shipbuilding, and other industries. Therefore, an understanding of the nonlinear and postbuckling responses of anisotropic panels is desirable.

The limited studies of anisotropic panels may be attributed to the high computational expense involved in the nonlinear analysis of these panels. As has been reported in the literature, anisotropy has an adverse effect on the accuracy and convergence of both numerical and analytic solutions (see, for example, Refs. 1-3). Moreover, the presence of anisotropy results in reducing the stiffness of the panel, thereby increasing the nonlinearity of the response.

In an attempt to reduce the cost of analyzing anisotropic panels, the different symmetries that exist in composite plates and shells having symmetric geometry, loading, and boundary conditions were identified in Refs. 4 and 5. Also, techniques have been developed in the cited references for exploiting these symmetries in the finite element analysis. However, in spite of these developments, the computational expense of analyzing highly anisotropic panels remains high, particularly in the presence of nonlinearities. Recently, a computational procedure was developed for reducing both the size of the analysis model and the total number of degrees of freedom used in the initial discretization of symmetric anisotropic panels.[6,7] In the cited references, displacement finite element models were used and the accuracy of the stress resultants was found to be considerably lower than that of displacements. The question arises as to whether a computational procedure can be developed for the nonlinear analysis of symmetric anisotropic structures that, in addition to reducing the size of the analysis model and the number of degrees of freedom, provides accurate stress resultants and displacements. The present study focuses on this question. Specifically, the objectives of this paper are: 1) to present a simple and efficient computational procedure for reducing both the size of the analysis model and the number of degrees of freedom used in the accurate prediction of the nonlinear response for symmetric anisotropic panels; and 2) to discuss the major advantages of the proposed procedure over the computational procedures based on displacement models reported previously in the literature.

The analytical formulation is based on a form of the geometrically nonlinear shallow shell theory with the effects of transverse shear deformation, anisotropic material behavior, and bending-extensional coupling included. The three key elements of the proposed computational procedure are: 1) use of three-field mixed models with independent interpolation functions for stress resultants, strain components, and generalized displacements; 2) operator splitting or decomposition of the material stiffness matrix of the shell into the sum of orthotropic and nonorthotropic parts; and 3) application of a two-parameter reduction method through the successive use of the finite element method and the classical Rayleigh-Ritz technique.

The use of the three-field mixed model simplifies the analytical development and improves the accuracy of stress predictions. The operator splitting allows the reduction of the size of the analysis model to that of the corresponding orthotropic structure and the application of reduction method results in substantial reduction in the total number of degrees of freedom. It is the combination of these three elements that leads to significant reduction in computational effort and is the new contribution of the present paper.

Mathematical Formulation

A total Lagrangian formulation is used and the panel is discretized by using a three-field, Hu-Washizu type mixed model. The fundamental unknowns consist of: the five generalized displacements u_α, w, and ϕ_α; the eight stress resultants $N_{\alpha\beta}$, $M_{\alpha\beta}$, and Q_α; and the corresponding eight strain components of the middle surface $\epsilon_{\alpha\beta}$, $\kappa_{\alpha\beta}$, and $2\epsilon_{\alpha 3}$ $(\alpha,\beta=1,2)$ (see Fig. 1 for sign convention).

The governing finite element equations are obtained by applying the Hu-Washizu variational principle (see Appendix A). The degree of the polynomial interpolation (or shape) functions used in approximating the strain components $\epsilon_{\alpha\beta}$, $\kappa_{\alpha\beta}$, and $2\epsilon_{\alpha 3}$ is the same as that used for approximating the corresponding stress resultants $N_{\alpha\beta}$, $M_{\alpha\beta}$, and Q_α and differs from the degree of interpolation functions used in approximating the generalized displacements u_α, w, and ϕ_α. Moreover, the continuity of the stress resultants and strain components is not imposed at the interelement boundaries and, therefore, both the strain parameters and stress-resultant parameters can be eliminated on the element level.

For the purpose of reducing the size of the analysis model for symmetric anisotropic structures, the material stiffness matrix of the shell is decomposed into the sum of orthotropic and nonorthotropic parts. The governing finite element equations for the individual elements are embedded in a two-parameter family of equations of the form,

$$f_\mathcal{I}^{(\Phi)}(\lambda,q)=\left(\Re_{\mathcal{I}\mathcal{J}}+\lambda\mathcal{K}_{\mathcal{I}\mathcal{J}}\right)\Phi_\mathcal{J}+R_{\mathcal{I}\mathcal{J}}H_\mathcal{J}=0 \quad (1)$$

$$f_\mathcal{I}^{(H)}(\lambda,q)=(R')_{\mathcal{I}\mathcal{J}}\Phi_\mathcal{J}+S_{\mathcal{I}J}X_J+\tfrac{1}{2}\mathfrak{M}_{\mathcal{I}JL}X_JX_L=0 \quad (2)$$

$$f_I^{(X)}(\lambda,q)=(S')_{I\mathcal{J}}H_\mathcal{J}+\mathfrak{M}_{\mathcal{L}IJ}X_JH_\mathcal{L}-qQ_I=0 \quad (3)$$

where X_I, Φ_J, and H_J are nodal displacements, strain, and stress-resultant parameters, respectively; the $\Re$, $\mathcal{K}$, R, and S terms generalized stiffness coefficients; Q_I are normalized consistent load coefficients; q is a load parameter; λ is a

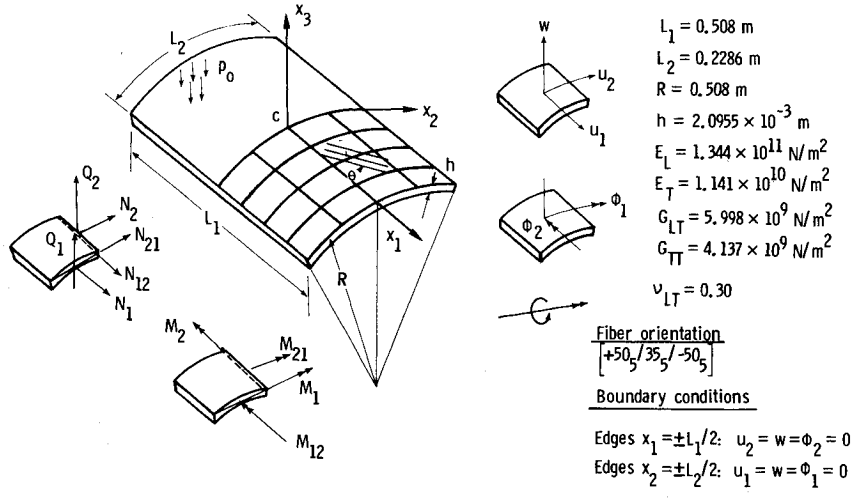

Fig. 1 Cylindrical panel used in the present study.

tracing parameter that identifies all the nonorthotropic (anisotropic) contributions in the elemental equations; the superscript t denotes transposition; and the array $\mathfrak{M}_{\mathscr{I}IJ}$ represents nonlinear contributions. The range of the uppercase script indices is 1-8 δ, where δ is the number of parameters used in approximating each of the stress resultants (or strain components); and the range of the uppercase Latin indices is 1-5 m (where m is the number of displacement nodes). A repeated index in the same term denotes summation over the full range of the index.

The form of the arrays $\mathfrak{K}$, $\mathscr{K}$, R, S, $\mathfrak{M}$, and Q is given in Refs. 8 and 9. Equations (1-3) represent the constitutive relations (stress resultants-strain relations), the strain-displacement relations, and the equilibrium equations for an individual element, respectively.

Application of Two-Parameter Reduction Method

Basic Idea of the Reduction Method

A two-parameter reduction method is applied to reduce both the size of the analysis model and the total number of degrees of freedom used in the initial discretization. The basic idea of the reduction method is to use the finite element method for the initial discretization and to express each of the vectors of nodal displacements, stress-resultant, and strain parameters as a linear combination of a small number of global approximation vectors (or modes). This is accomplished by using the following transformations:

$$\Phi_{\mathscr{I}} = \Gamma^{(\Phi)}_{\mathscr{I}i}\psi_i \tag{4}$$

$$H_{\mathscr{I}} = \Gamma^{(H)}_{\mathscr{I}i}\psi_i \tag{5}$$

$$X_I = \Gamma^{(X)}_{Ii}\psi_i, \quad i = 1\text{-}r \tag{6}$$

where ψ_i ($i = 1$-r) is a vector of undetermined coefficients (amplitudes of global modes), which are functions of λ and q; $\Gamma^{(\Phi)}$, $\Gamma^{(H)}$, $\Gamma^{(X)}$ transformation matrices whose columns are the global approximation vectors; and r is the number of global approximation vectors.

The application of the reduction method can be conveniently divided into the following two distinct steps: 1) generation of global approximation vectors (or modes) using the finite element method; and 2) computation of the amplitudes of the approximation vectors via the classical Rayleigh-Ritz technique. The two steps are described below.

Generation of Global Approximation Vectors

An effective choice for the global approximation vectors was found to consist of the nonlinear solution and its various order derivatives with respect to λ and q. The equations used in generating these vectors are obtained by successive differentiation of the finite element equations of the discretized panel [Eqs. (1-3)] and are listed in Appendix B. For convenience, the initial set of global approximation vectors is generated at $\lambda = q = 0$. This results in reducing the computational effort in evaluating the global approximation vectors because: 1) for $q = 0$, $\Phi_{\mathscr{I}} = 0$, $H_{\mathscr{I}} = 0$, $X_I = 0$, and all the nonlinear terms on the left-hand sides of the equations drop out; and 2) for $\lambda = 0$, each of the global approximation vectors exhibits the same types of symmetries (or antisymmetries) as those exhibited by orthotropic panels and, therefore, the size of the model used in generating these vectors is the same as that used for orthotropic panels.

The criterion for selecting the number of basis vectors proposed in Ref. 8 was adopted in the present study. The criterion is based on monitoring the condition number of the Gram matrix $\bar{\beta}$ of the global approximation vectors and terminating the generation of these vectors when $\bar{\beta}$ exceeds a prescribed value. Also, upper and lower limits of global approximation vectors were chosen to be 3 and 21, respectively.

Computation of Amplitudes of Global Approximation Vectors

A classical Rayleigh-Ritz technique is used to replace Eqs. (1-3) by the following system of nonlinear equations in the unknown parameters ψ_i:

$$f_i^{(\psi)}(\lambda, q) = \left(\tilde{\mathfrak{k}}_{ij} + \lambda\tilde{\mathscr{k}}_{ij}\right)\psi_j + \tilde{\mathfrak{m}}_{ijk}\psi_j\psi_k - q\tilde{\mathscr{Q}}_i = 0 \tag{7}$$

where

$$\tilde{\mathfrak{k}}_{ij} = \sum_{\text{elements}} \Big[\mathfrak{K}_{\mathscr{I}\mathscr{J}}\Gamma^{(\Phi)}_{\mathscr{I}i}\Gamma^{(\Phi)}_{\mathscr{J}j} + R_{\mathscr{I}\mathscr{J}}\Gamma^{(\Phi)}_{\mathscr{I}i}\Gamma^{(H)}_{\mathscr{J}j} + (R^t)_{\mathscr{I}\mathscr{J}}\Gamma^{(H)}_{\mathscr{I}i}\Gamma^{(\Phi)}_{\mathscr{J}j} + S_{\mathscr{I}J}\Gamma^{(H)}_{\mathscr{I}i}\Gamma^{(X)}_{Jj} + (S^t)_{I\mathscr{J}}\Gamma^{(X)}_{Ii}\Gamma^{(H)}_{\mathscr{J}j}\Big] \tag{8}$$

$$\tilde{\mathscr{k}}_{ij} = \sum_{\text{elements}} \mathscr{K}_{\mathscr{I}\mathscr{J}}\Gamma^{(\Phi)}_{\mathscr{I}i}\Gamma^{(\Phi)}_{\mathscr{J}j} \tag{9}$$

$$\tilde{\mathfrak{m}}_{ijk} = \sum_{\text{elements}} \tfrac{1}{2}\mathfrak{M}_{\mathscr{I}JK}\Big[\Gamma^{(H)}_{\mathscr{I}i}\Gamma^{(X)}_{Jj}\Gamma^{(X)}_{Kk} + \Gamma^{(H)}_{\mathscr{J}j}\Gamma^{(X)}_{Jk}\Gamma^{(X)}_{Ki} + \Gamma^{(H)}_{\mathscr{J}k}\Gamma^{(X)}_{Ji}\Gamma^{(X)}_{Kj}\Big] \tag{10}$$

$$\tilde{\mathscr{Q}}_i = \sum_{\text{elements}} \Gamma^{(X)}_{Ji}Q_J \tag{11}$$

In Eqs. (7-11), a repeated subscript in the same term denotes summation over its full range. Indices between parentheses are not summed.

If the reduced equations of the mixed model [Eqs. (7)] are contrasted with those of the displacement model presented in Ref. 7, the following can be noted:

1) The mixed equations are quadratic in the reduced unknowns ψ_i, whereas the corresponding displacement equations are cubic in ψ_i.

2) The nonorthotropic contributions are *all* contained in the two-dimensional array $\tilde{\mathscr{k}}_{ij}$. By contrast, in the displacement equations nonorthotropic contributions *are included also in the three- and four-dimensional arrays.*

3) In view of the explicit approximation of $\Phi_{\mathscr{I}}$ and $H_{\mathscr{I}}$ in the mixed equations (through the use of $\Gamma^{(\Phi)}_{\mathscr{I}i}$ and $\Gamma^{(H)}_{\mathscr{I}i}$), the mixed equations are expected to provide better approximation for the stress resultants and strain components than those of the displacement models.

Sensitivity of the Nonlinear Response of the Structure to Nonorthotropic Material Coefficients

The chosen set of global approximation vectors provides a direct measure of the sensitivity of the different response quantities to nonorthotropic (anisotropic) material coefficients of the structure. Moreover, the global approximation vectors can be used to compute the derivatives of the total strain energy U with respect to λ. The expressions of the first three derivatives of U are

$$\left.\frac{\partial U}{\partial\lambda}\right|_0 = \mathfrak{K}_{\mathscr{I}\mathscr{J}}\Phi_{\mathscr{I}}\frac{\partial\Phi_{\mathscr{J}}}{\partial\lambda} + \frac{1}{2}\mathscr{K}_{\mathscr{I}\mathscr{J}}\Phi_{\mathscr{I}}\Phi_{\mathscr{J}} \tag{12}$$

$$\left.\frac{\partial^2 U}{\partial\lambda^2}\right|_0 = \mathfrak{K}_{\mathscr{I}\mathscr{J}}\left(\Phi_{\mathscr{I}}\frac{\partial^2\Phi_{\mathscr{J}}}{\partial\lambda^2} + \frac{\partial\Phi_{\mathscr{I}}}{\partial\lambda}\frac{\partial\Phi_{\mathscr{J}}}{\partial\lambda}\right) + 2\mathscr{K}_{\mathscr{I}\mathscr{J}}\Phi_{\mathscr{I}}\frac{\partial\Phi_{\mathscr{J}}}{\partial\lambda} \tag{13}$$

$$\left.\frac{\partial^3 U}{\partial\lambda^3}\right|_0 = \mathfrak{K}_{\mathscr{I}\mathscr{J}}\left(\Phi_{\mathscr{I}}\frac{\partial^3\Phi_{\mathscr{J}}}{\partial\lambda^3} + 3\frac{\partial\Phi_{\mathscr{I}}}{\partial\lambda}\frac{\partial^2\Phi_{\mathscr{J}}}{\partial\lambda^2}\right) + 3\mathscr{K}_{\mathscr{I}\mathscr{J}}\left(\Phi_{\mathscr{I}}\frac{\partial^2\Phi_{\mathscr{J}}}{\partial\lambda^2} + \frac{\partial\Phi_{\mathscr{I}}}{\partial\lambda}\frac{\partial\Phi_{\mathscr{J}}}{\partial\lambda}\right) \tag{14}$$

$$\left.\frac{\partial^4 U}{\partial\lambda^4}\right|_0 = \Re_{\mathscr{J}\mathscr{J}}\left(\Phi_{\mathscr{J}}\frac{\partial^4\Phi_{\mathscr{J}}}{\partial\lambda^4}+4\frac{\partial\Phi_{\mathscr{J}}}{\partial\lambda}\frac{\partial^3\Phi_{\mathscr{J}}}{\partial\lambda^3}+3\frac{\partial^2\Phi_{\mathscr{J}}}{\partial\lambda^2}\frac{\partial^2\Phi_{\mathscr{J}}}{\partial\lambda^2}\right)$$

$$+4\mathscr{K}_{\mathscr{J}\mathscr{J}}\left(\Phi_{\mathscr{J}}\frac{\partial^3\Phi_{\mathscr{J}}}{\partial\lambda^3}+3\frac{\partial\Phi_{\mathscr{J}}}{\partial\lambda}\frac{\partial^2\Phi_{\mathscr{J}}}{\partial\lambda^2}\right) \tag{15}$$

The derivatives of U in Eqs. (12-15) can be used as quantitative measures for the sensitivity of the global response of the structure to the nonorthotropic material coefficients. Specifically, dimensionless parameters ρ_ℓ are introduced such that

$$\rho_\ell = \left.\frac{\partial^\ell U}{\partial\lambda^\ell}\right|_0 \Big/ U_0 \quad (\ell \text{ is not summed}) \tag{16}$$

where

$$U_0 = \tfrac{1}{2}\Re_{\mathscr{J}\mathscr{J}}\Phi_{\mathscr{J}}\Phi_{\mathscr{J}} \tag{17}$$

The smaller the values of ρ_ℓ the less sensitive the response is to the nonorthotropic material coefficients of the structure and vice versa. Also, small values of ρ_ℓ (less than 0.05) indicate that only few global approximation vectors are needed for approximating the response of the anisotropic structure and that Taylor series expansion can provide an acceptable approximation for the response. On the other hand, large values of ρ_ℓ (greater than 0.20) indicate that more global approximation vectors are needed for approximating the response. All the terms on the right-hand sides of Eqs. (12-15), apart from a numerical coefficient, are identical to the coefficients of the reduced arrays.

Note that at $q=0$, $\Phi_{\mathscr{J}}=0$, $U_0=0$, and all the sensitivity derivatives in Eqs. (12-15) are zero. To obtain a quantitative measure of the sensitivity of the global response to the nonorthotropic material coefficients at $q=0$, the following substitutions must be made in Eqs. (12-17):

$$\frac{\partial^{n+1}\Phi_{\mathscr{J}}}{\partial q\,\partial\lambda^n} \quad \text{for} \quad \frac{\partial^n\Phi_{\mathscr{J}}}{\partial\lambda^n} \quad \text{where } n=0,1,2,3,4$$

This amounts to replacing the sensitivity derivatives in Eqs. (12-15)

$$\left.\frac{\partial^n U}{\partial\lambda^n}\right|_0, \quad \text{by} \quad \frac{1}{2}\left.\frac{\partial^{n+2}U}{\partial q^2\,\partial\lambda^n}\right|_0$$

Numerical Studies

To assess the effectiveness of the proposed computational procedure, a number of nonlinear problems of symmetric anisotropic panels have been solved by using this procedure. For each problem, the solutions obtained by the proposed procedure were compared with the direct solution of the anisotropic panel. Herein the solutions for a typical problem of a 15-ply cylindrical panel subjected to uniform normal loading are discussed. The panel is made of graphite-epoxy material and, to amplify the effect of anisotropy, the fiber orientation is assumed to be $[+50_5/35_5/-50_5]$ (see Fig. 1). The numerical results are summarized in Figs. 2-5 and in Tables 1 and 2. As expected, the normal displacement w, the stress resultants $N_{\alpha\beta}$, $M_{\alpha\beta}$, and the strain components $\epsilon_{\alpha\beta}$ and $\kappa_{\alpha\beta}$ exhibit inversion symmetry. The in-plane displacements

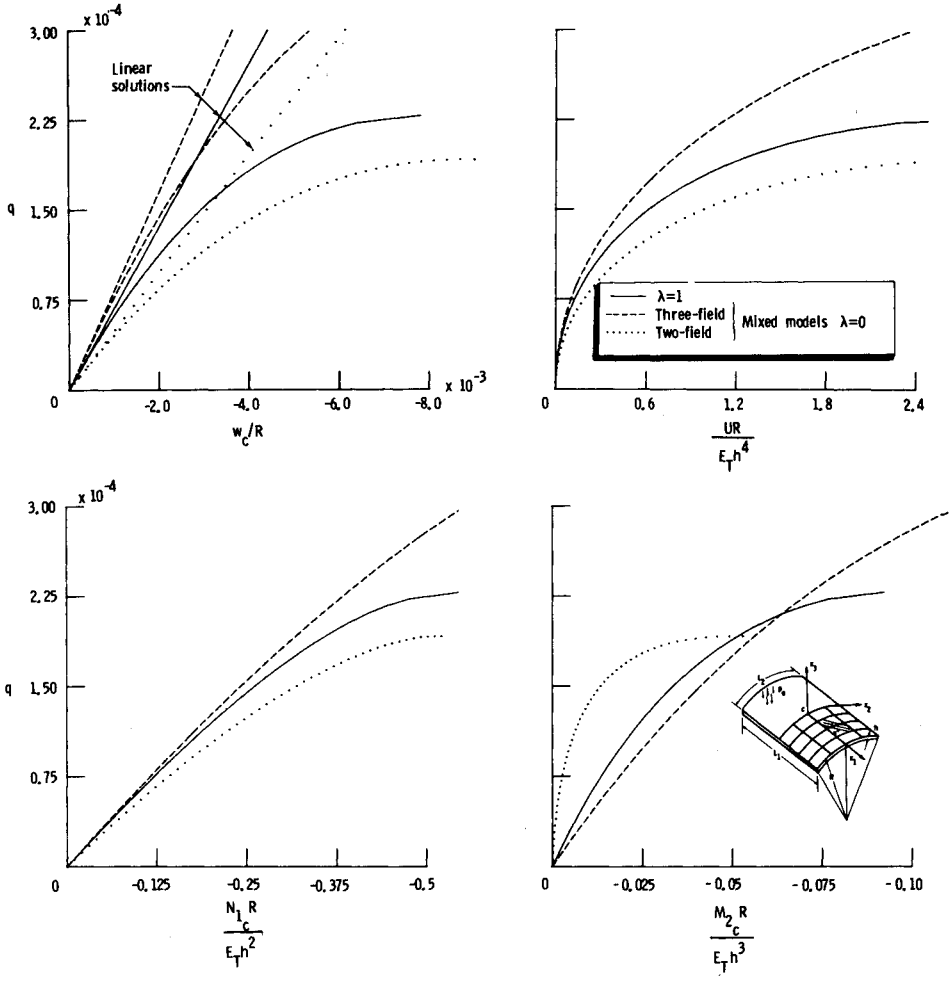

Fig. 2 Nonlinear response of anisotropic cylindrical panel subjected to uniform normal loading (see Fig. 1).

u_α, the rotation components ϕ_α, the transverse shear stress resultants Q_α, and the transverse shear strains $2\epsilon_{\alpha 3}$ exhibit inversion antisymmetry. These symmetry properties were used in conjunction with the procedure outlined in Ref. 4 to reduce the analysis model to half the shell. A 6×6 uniform grid of mixed elements was used. Both three- and two-field mixed models were developed. Biquadratic interpolation functions were used for approximating each of the generalized displacements, and bilinear interpolation functions were used for approximating each of the stress resultants and strain components (a total of 699 nonzero displacement degrees of freedom, 1152 stress-resultant parameters, and 1152 strain parameters). Gauss-Legendre quadrature formulas with four quadrature points in the element domain were used for the evaluation of the elemental arrays.

The highly anisotropic response of the panel is depicted in Figs. 2 and 3. Figure 2 shows the variations of the normal displacement w_c, the total strain energy U, and the stress resultants N_{1c} and M_{2c} with the loading parameter $q = p_0 R/E_T h$; for the two cases, $\lambda = 1$ (anisotropic panel) and $\lambda = 0$ (nonorthotropic arrays set equal to zero). For the case $\lambda = 1$, the solutions obtained using the three- and two-field mixed models were identical. This is a direct consequence of the equivalence between the two models noted in Ref. 8. However, for the case $\lambda = 0$, the shell response predicted by the three-field mixed models was stiffer and that of the two-field mixed models was more flexible than the case $\lambda = 1$. This difference in behavior is a result of the difference between decomposing the material stiffness and material flexibility matrices in the three- and two-field mixed models, respectively.

Figure 3 shows contour plots for the generalized displacements obtained by direct solution of the anisotropic shell at $q = 2.17 \times 10^{-4}$.

The analysis of the panel by the proposed technique was accomplished by applying the two-parameter reduction method. The global approximation vectors were generated at $q = 0$ and $\lambda = 0$ and were used to generate the solution corresponding to $\lambda = 1$ for various values of q.

The global approximation vectors exhibit symmetry (and/or antisymmetry) with respect to the two axes of symmetry of the shell. These symmetry relations are depicted in Fig. 4. The symmetry relations for the generalized displacements and stress resultants can be represented as follows:

$$\frac{\partial^{m+n}}{\partial q^m \partial \lambda^n}\begin{Bmatrix} u_1 \\ u_2 \\ w \\ \phi_1 \\ \phi_2 \end{Bmatrix}_{(x_1, x_2)} = \frac{\partial^{m+n}}{\partial q^m \partial \lambda^n}\begin{Bmatrix} -(-1)^n u_1 \\ (-1)^n u_2 \\ (-1)^n w \\ -(-1)^n \phi_1 \\ (-1)^n \phi_2 \end{Bmatrix}_{(-x_1, x_2)}$$

$$= \frac{\partial^{m+n}}{\partial q^m \partial \lambda^n}\begin{Bmatrix} (-1)^n u_1 \\ -(-1)^n u_2 \\ (-1)^n w \\ (-1)^n \phi_1 \\ -(-1)^n \phi_2 \end{Bmatrix}_{(x_1, -x_2)} \tag{18}$$

$$\frac{\partial^{m+n}}{\partial q^m \partial \lambda^n}\begin{Bmatrix} N_1 \\ N_2 \\ N_{12} \\ M_1 \\ M_2 \\ M_{12} \\ Q_1 \\ Q_2 \end{Bmatrix}_{(x_1, x_2)} = \frac{\partial^{m+n}}{\partial q^m \partial \lambda^n}\begin{Bmatrix} (-1)^n N_1 \\ (-1)^n N_2 \\ -(-1)^n N_{12} \\ (-1)^n M_1 \\ (-1)^n M_2 \\ -(-1)^n M_{12} \\ -(-1)^n Q_1 \\ (-1)^n Q_2 \end{Bmatrix}_{(-x_1, x_2)}$$

$$= \frac{\partial^{m+n}}{\partial q^m \partial \lambda^n}\begin{Bmatrix} (-1)^n N_1 \\ (-1)^n N_2 \\ -(-1)^n N_{12} \\ (-1)^n M_1 \\ (-1)^n M_2 \\ -(-1)^n M_{12} \\ (-1)^n Q_1 \\ -(-1)^n Q_2 \end{Bmatrix}_{(x_1, -x_2)} \tag{19}$$

where $n = 0, 1, 2, \ldots$. The maximum absolute values of the generalized displacements and their derivatives are given in Table 1. The symmetry relations for the strain components are the same as those for the corresponding stress resultants.

The symmetry relations [Eqs. (18) and (19)] clearly demonstrate the fact that the global approximation vectors can each be obtained by analyzing only one quadrant of the shell.

An indication of the accuracy and convergence of the solutions obtained by the proposed procedure is given in Fig. 5 and Table 2. The standard of comparison is taken to be the direct nonlinear finite element solution of the anisotropic shell. As can be seen from Fig. 5 and Table 2, the solutions obtained by the proposed procedure are highly accurate. At $q = 2.17 \times 10^{-4}$, the errors in the normal displacement w_c, strain energy U, and the stress resultants N_{1_c} and M_{2_c} obtained by using 15 global approximation vectors (all the nonzero derivatives with respect to q and λ of the order of five or less) were 0.5, 2, 3, and 3.2%, respectively. The corresponding errors obtained by using 21 vectors (all nonzero derivatives up to the order of six) were only 0, 0.1, 0.2, and 0.5%.

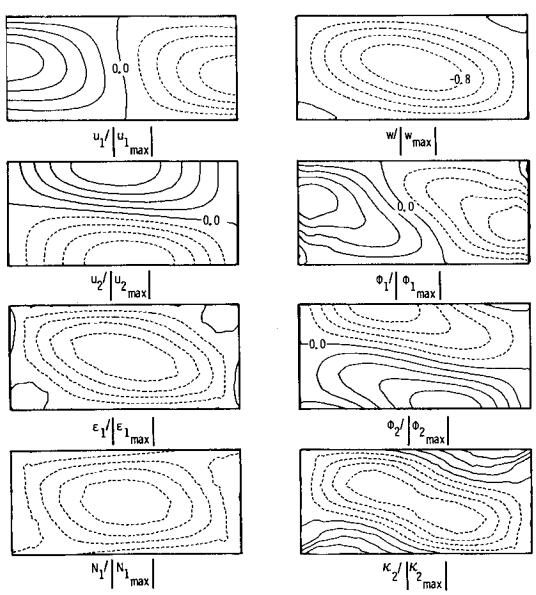

Fig. 3 Normalized contour plots for generalized displacements, strain components, and stress resultants. Anisotropic cylindrical panel subjected to uniform normal loading, $q = 2.17 \times 10^{-4}$ (see Fig. 1); dashed lines represent negative contours.

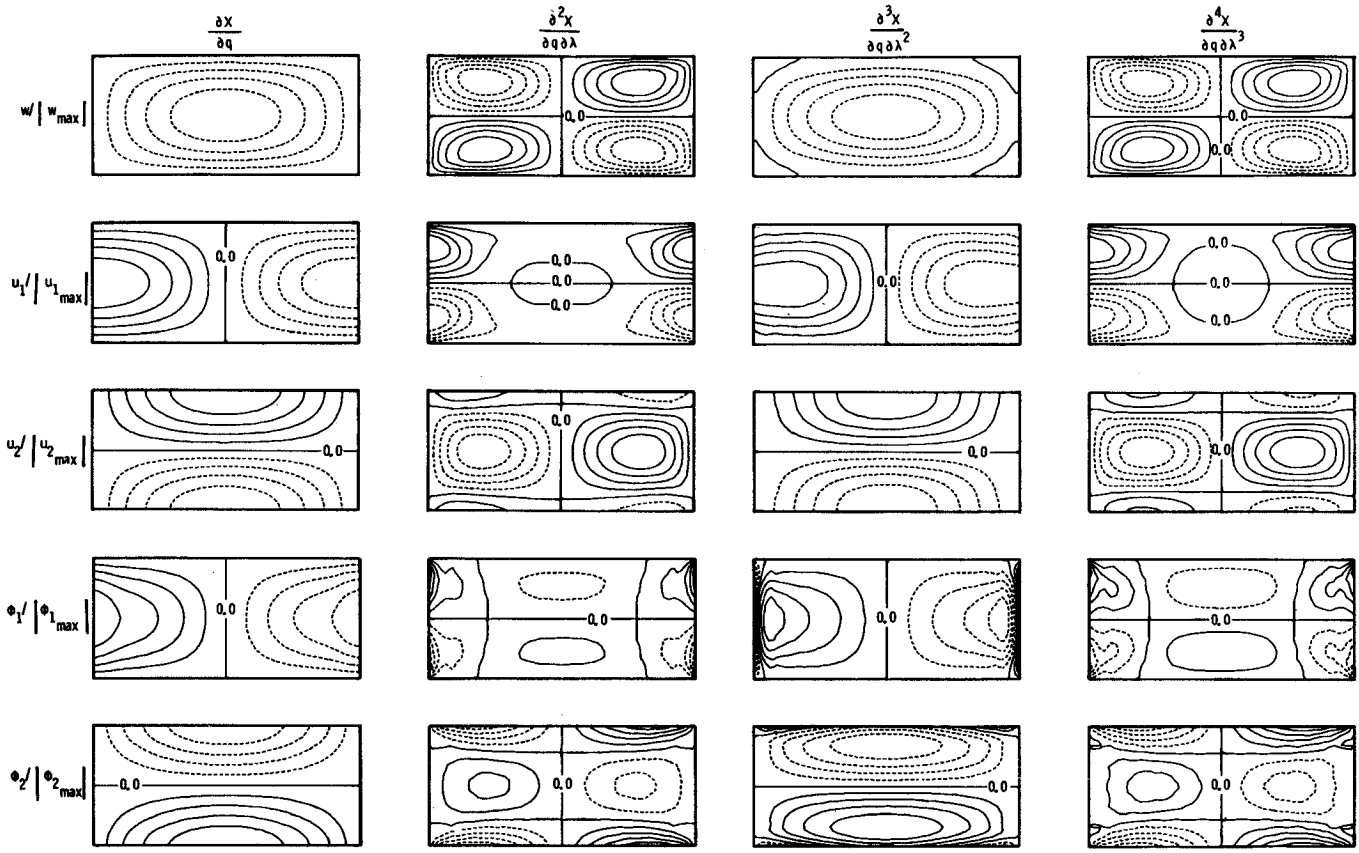

Fig. 4 Normalized contour plots for global approximation vectors. Anisotropic cylindrical shell subjected to uniform normal loading (see Fig. 1); dashed lines represent negative contours.

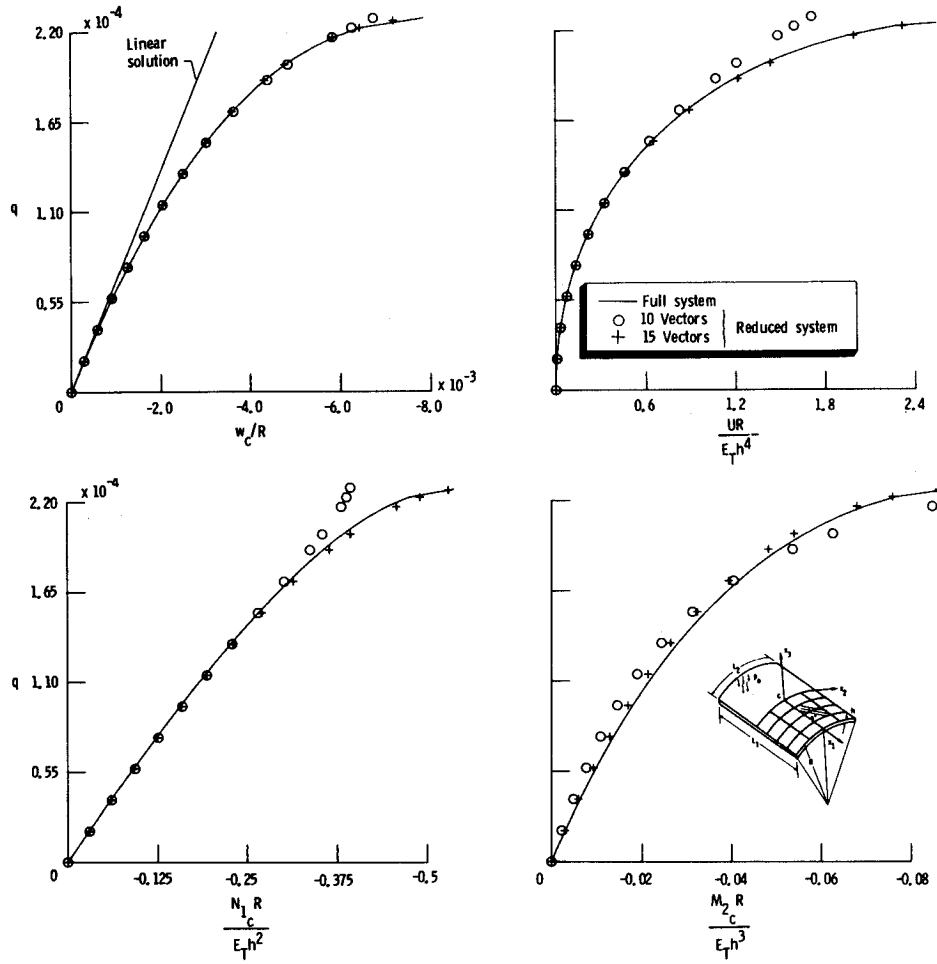

Fig. 5 Accuracy of solutions obtained by proposed computational procedure. Anisotropic cylindrical panel subjected to uniform loading (see Fig. 1).

Table 1 Maximum absolute values of generalized displacements and their derivatives, evaluated at $q = \lambda = 0$[a]

	$\left\{\frac{\partial X}{\partial q}\right\}_0$	$\left\{\frac{\partial^2 X}{\partial q\,\partial\lambda}\right\}_0$	$\left\{\frac{\partial^3 X}{\partial q\,\partial\lambda^2}\right\}_0$	$\left\{\frac{\partial^4 X}{\partial q\,\partial\lambda^3}\right\}_0$
$10^{-4}\times u_1 E_T/h$	4.404	0.332	0.722	0.780
$10^{-4}\times u_2 E_T/h$	11.788	0.778	2.829	1.495
$10^{-4}\times wE_T/h$	71.881	5.071	19.856	12.837
$10^{-4}\times \phi_1 L_2 E_T/h$	117.964	42.054	36.681	76.755
$10^{-4}\times \phi_2 L_2 E_T/h$	252.186	56.429	60.461	136.050

[a]Anisotropic cylindrical panel subjected to uniform normal loading (see Fig. 1).

Table 2 Accuracy and convergence of solutions obtained by proposed procedure with increasing number of global approximation vectors[a]

r	$-10^3\times\frac{w_c}{R}$	$\frac{UR}{E_T h^4}$	$-10\times\frac{N_{1_c}R}{E_T h^2}$	$-10^2\times\frac{M_{2_c}R}{E_T h^3}$
10	5.833	1.4875	3.814	8.469
15	5.842	1.9936	4.584	6.786
21	5.873	1.9560	4.443	6.977
Full system	5.872	1.9543	4.449	7.011

[a] Anisotropic cylindrical panel subjected to uniform normal loading (see Fig. 1), $q = 2.17\times10^{-4}$.

Conclusions

A computational procedure is presented for the efficient analysis of symmetric anisotropic structures. The three key elements of the procedure are: 1) use of three-field mixed models having independent interpolation (shape) functions for strain components, stress resultants, and generalized displacements with the strain components and stress resultants allowed to be discontinuous at interelement boundaries; 2) operator splitting or decomposition of the material stiffness matrix into the sum of an orthotropic and a nonorthotropic (anisotropic) parts; and 3) application of a reduction method, through the successive use of the finite element method and the classical Rayleigh-Ritz technique. The finite element method is first used to generate a few global approximation vectors (or modes). Then the amplitudes of these modes are computed by using the classical Rayleigh-Ritz technique. The global approximation vectors are taken to be the various-order derivatives of the strain components, stress resultants, and generalized displacements with respect to two parameters, namely: anisotropic tracing parameter identifying all the nonorthotropic terms in the material stiffness matrix; and load or arc-length parameter in the solution space. The approximation vectors are evaluated at zero values of the two parameters and, therefore, the size of the analysis model used in their generation is identical to that of the corresponding orthotropic structure.

Numerical example of the nonlinear response of an anisotropic cylindrical panel subjected to uniform normal loading is used to demonstrate the effectiveness of the proposed reduction method. The results of the study suggest the following conclusions relative to the use of the three-field mixed models, the selection of global approximation vectors, and the potential of the proposed computational procedure:

1) The use of the three-field mixed models enhances the effectiveness of the foregoing computational procedure, and offers the following advantages over the equivalent reduced-integration displacement models[7]:

a) For model-size reduction of symmetric anisotropic structures, the decomposition of the material stiffness matrix of the shell affects only the linear arrays $\mathfrak{R}_{\mathscr{J}\mathscr{J}}$ and $\mathscr{K}_{\mathscr{J}\mathscr{J}}$. By contrast, if a displacement model is used, both linear and nonlinear arrays are affected by the decomposition (see Ref. 7).

b) The generation of the global approximation vectors is easier and involves fewer arithmetic operations than in the displacement formulation. This is because the nonlinear terms of the mixed models are bilinear (or quadratic) in the nodal displacements and the stress-resultant parameters are not cubic as in the displacement formulation.

c) For a given number of global approximation vectors the accuracy of the solutions obtained by the reduced three-field mixed models is higher than that obtained by the reduced-integration displacement approach.[7] This is particularly true for stress resultants and strain components.

2) The use of path derivatives as global approximation vectors leads to accurate solutions with a small number of vectors. Therefore, the time required to solve the reduced equations is relatively small and the total analysis time to a first approximation equals the time required to evaluate the global approximation vectors and to generate the reduced equations. The operator splitting technique allows the reduction of the size of the analysis model to that of the corresponding orthotropic structure and, therefore, the time of generating the global approximation vectors is reduced.

3) The global approximation vectors provide a direct measure of the sensitivity of the different response quantities to the nonorthotropic (anisotropic) material coefficients of the structure. The sensitivity of the global response can also be assessed by using these vectors.

4) The two-parameter reduction method exploits the best elements of the finite element method and the Rayleigh-Ritz technique as follows:

a) The finite element method is used as a general approach for generating global approximation vectors. The size of the analysis model used in generating these vectors is the same as that of the corresponding orthotropic panel.

b) The Rayleigh-Ritz technique is used as an efficient procedure for minimizing and distributing the error throughout the structure.

5) The reduction method extends the range of applicability of the Taylor series expansion by relaxing the requirement of using small parameters λ and q in the expansion.

Appendix A: Three-Field Mixed Variational Principle and Finite Element Discretization

A total Lagrangian description of the shell deformation is used and the panel configurations at different load levels are referred to the initial coordinate system of the undeformed panel.

Variational Principle

The functional used in the development of three-field, Hu-Washizu type mixed finite element models has the following form:

$$\pi\left(\epsilon_{\alpha\beta}, \kappa_{\alpha\beta}, 2\epsilon_{\alpha 3}, N_{\alpha\beta}, M_{\alpha\beta}, Q_\alpha, u_\alpha, w, \phi_\alpha\right) = U - V - W - W^\sigma - W^u \tag{A1}$$

where

$$U=\int_{\Omega}\frac{1}{2}\left[C_{\alpha\beta\gamma\rho}\epsilon_{\alpha\beta}\epsilon_{\gamma\rho}+2F_{\alpha\beta\gamma\rho}\epsilon_{\alpha\beta}\kappa_{\gamma\rho}+D_{\alpha\beta\gamma\rho}\kappa_{\alpha\beta}\kappa_{\gamma\rho}+C_{\alpha3\beta3}(2\epsilon_{\alpha3})(2\epsilon_{\beta3})\right]\mathrm{d}\Omega \tag{A2}$$

$$V=\int_{\Omega}\Big\{N_{\alpha\beta}\Big[\epsilon_{\alpha\beta}-\frac{1}{2}(\partial_\alpha u_\beta+\partial_\beta u_\alpha+2k_{\alpha\beta}w+\partial_\alpha w\partial_\beta w)\Big]+M_{\alpha\beta}\Big[\kappa_{\alpha\beta}-\frac{1}{2}(\partial_\alpha\phi_\beta+\partial_\beta\phi_\alpha)\Big]+Q_\alpha[2\epsilon_{\alpha3}-(\phi_\alpha+\partial_\alpha w)]\Big\}\mathrm{d}\Omega \tag{A3}$$

$$W=\int_{\Omega}(p_\alpha u_\alpha+pw)\,\mathrm{d}\Omega \tag{A4}$$

$$W^{\sigma}=\int_{c_\sigma}\left[\tilde{N}_{\alpha\beta}u_\beta+(\tilde{Q}_\alpha+\tilde{N}_{\alpha\beta}\partial_\beta w)w+\tilde{M}_{\alpha\beta}\phi_\beta\right]n_\alpha\,\mathrm{d}c \tag{A5}$$

$$W^{u}=\int_{c_u}\left[N_{\alpha\beta}(u_\beta-\tilde{u}_\beta)+(Q_\alpha+N_{\alpha\beta}\partial_\beta w)(w-\tilde{w})+M_{\alpha\beta}(\phi_\beta-\tilde{\phi}_\beta)\right]n_\alpha\,\mathrm{d}c \tag{A6}$$

In Eqs. (A1-A6), U is the strain energy of the shell, $\epsilon_{\alpha\beta}$ and $\kappa_{\alpha\beta}$ the extensional and bending strains of the shell middle surface, $2\epsilon_{\alpha3}$ the transverse shear strains, u_α and w the displacement components in the x_α and x_3 coordinate directions, ϕ_α the rotation components, p_α and p the intensities of external loads in the x_α and x_3 coordinate directions, $C_{\alpha\beta\gamma\rho}$ and $D_{\alpha\beta\gamma\rho}$ the extensional and bending stiffnesses of the shell, $F_{\alpha\beta\gamma\rho}$ bending-extensional coupling coefficients of the shell, Ω the shell domain, c_σ and c_u the portions of the shell boundary over which stress resultants and displacements are prescribed, $k_{\alpha\beta}$ the curvatures and twist of the middle surface of the shell, and n_α the unit outward normal to the shell boundary. Quantities with a tilde ($\tilde{}$) denote prescribed displacements and stress resultants, $\partial_\alpha\equiv\partial/\partial x_\alpha$, the range of the Greek subscripts is 1,2, and a repeated subscript in the same term denotes summation.

Finite Element Discretization

The finite element discretization is performed by decomposing the shell region into finite elements $\Omega^{(e)}$ and approximating the strain components; stress resultants and generalized displacements within each element by expressions of the form

$$u_\alpha=\mathcal{N}^i X^i_\alpha \tag{A7}$$

$$w=\mathcal{N}^i X^i_3 \tag{A8}$$

$$\phi_\alpha=\mathcal{N}^i X^i_{3+\alpha} \tag{A9}$$

$$N_{\alpha\beta}=\bar{\mathcal{N}}^i H^i_{\alpha+\beta-1} \tag{A10}$$

$$M_{\alpha\beta}=\bar{\mathcal{N}}^i H^i_{\alpha+\beta+2} \tag{A11}$$

$$Q_\alpha=\bar{\mathcal{N}}^i H^i_{\alpha+6} \tag{A12}$$

$$\epsilon_{\alpha\beta}=\bar{\mathcal{N}}^i \Phi^i_{\alpha+\beta-1} \tag{A13}$$

$$\kappa_{\alpha\beta}=\bar{\mathcal{N}}^i \Phi^i_{\alpha+\beta+2} \tag{A14}$$

$$2\epsilon_{\alpha3}=\bar{\mathcal{N}}^i \Phi^i_{\alpha+6} \tag{A15}$$

where $\mathcal{N}^i$ and $\bar{\mathcal{N}}^i$ are the shape functions used in approximating the generalized displacements and the stress resultants (and strain components), X the nodal displacements, and H and Φ the stress-resultant and strain parameters, respectively.

The finite element equations for individual elements are obtained by first replacing the generalized displacements, stress resultants, and strain components by their expressions in terms of the shape functions and then applying the stationary condition of the functional π, namely,

$$\delta\pi=0 \tag{A16}$$

If the parameters Φ, H, and X are varied independently and simultaneously, one obtains the three sets of governing finite element equations (1-3), namely, the constitutive relations, the strain-displacement relations, and the equilibrium equations.

Appendix B: Evaluation of Global Approximation Vectors

The global approximation vectors in Eqs. (4-6) are obtained by successive differentiation of the governing finite element equations (1-3) with respect to the two parameters q and λ and solving the resulting system of linear simultaneous algebraic equations. For individual finite elements, the recursion formulas for the global approximation vectors can be written in the following compact form:

$$\begin{bmatrix} \Re_{\mathcal{I}\mathcal{J}} & R_{\mathcal{I}\mathcal{J}} & 0 \\ (R^t)_{\mathcal{I}\mathcal{J}} & 0 & S_{\mathcal{I}J}+\mathfrak{M}_{\mathcal{I}JL}X_L \\ 0 & (S^t)_{I\mathcal{J}}+\mathfrak{M}_{IJ\mathcal{J}}X_J & \mathfrak{M}_{\mathcal{L}IJ}H_{\mathcal{L}} \end{bmatrix} \times\frac{\partial^{m+n}}{\partial q^m\,\partial\lambda^n}\begin{Bmatrix}\Phi_{\mathcal{J}}\\ H_{\mathcal{J}}\\ X_J\end{Bmatrix}=-\begin{Bmatrix}\mathfrak{G}^{(m+n)}_{\mathcal{I}}\\ \Re^{(m+n)}_{\mathcal{I}}\\ \mathfrak{Q}^{(m+n)}_{I}\end{Bmatrix} \tag{B1}$$

where the range of uppercase script indices is 1 to 8 σ (σ is the number of parameters used in approximating each of the stress resultants or strain components), the range of the uppercase Latin indices is 1-5 m (m is the number of displacement nodes), and a repeated subscript in the same term denotes summation over the full range of the subscript. The total number of $(m+n)$ combinations is $(r-1)$, where r is the number of approximation vectors. The explicit form of the components of the first few right-hand sides, $\mathfrak{G}^{(m+n)}_{\mathcal{I}}$, $\Re^{(m+n)}_{\mathcal{I}}$, and $\mathfrak{Q}^{(m+n)}_{I}$ are given in Table B1.

In Table B1 a dot ($\dot{}$) over a symbol refers to a derivative with respect to q and a prime ($'$) over a symbol refers to a derivative with respect to λ.

Note that the coefficient matrix on the left-hand side of Eqs. (B1), which must be factored, is the same for each of the

Table B1 Explicit forms of $\mathfrak{G}_{\mathscr{J}}^{(m+n)}$, $\mathfrak{R}_{\mathscr{J}}^{(m+n)}$, and $\mathfrak{Q}_{\mathscr{J}}^{(m+n)}$

$m+n$	m	n	$\mathfrak{G}_{\mathscr{J}}^{(m+n)}$	$\mathfrak{R}_{\mathscr{J}}^{(m+n)}$	$\mathfrak{Q}_{\mathscr{J}}^{(m+n)}$
1	1	0	0	0	Q_I
	0	1	$\mathscr{K}_{\mathscr{J}\mathscr{J}}\Phi_{\mathscr{J}}$	0	0
2	2	0	0	$\mathfrak{M}_{\mathscr{J}JL}\dot{X}_J\dot{X}_L$	$2\mathfrak{M}_{\mathscr{L}IJ}\dot{X}_J\dot{H}_{\mathscr{L}}$
	1	1	$\mathscr{K}_{\mathscr{J}\mathscr{J}}\dot{\Phi}_{\mathscr{J}}$	$\mathfrak{M}_{\mathscr{J}JL}\dot{X}_J\dot{X}_L$	$\mathfrak{M}_{\mathscr{L}IJ}(\dot{X}_J\dot{H}_{\mathscr{L}}+\dot{X}_J\dot{H}_{\mathscr{L}})$
	0	2	$2\mathscr{K}_{\mathscr{J}\mathscr{J}}\dot{\Phi}_{\mathscr{J}}$	$\mathfrak{M}_{\mathscr{J}JL}\dot{X}_J\dot{X}_L$	$2\mathfrak{M}_{\mathscr{L}IJ}\dot{X}_J\dot{H}_{\mathscr{L}}$
3	3	0	0	$3\mathfrak{M}_{\mathscr{J}JL}\ddot{X}_J\dot{X}_L$	$3\mathfrak{M}_{\mathscr{L}IJ}(\ddot{X}_J\dot{H}_{\mathscr{L}}+\dot{X}_J\ddot{H}_{\mathscr{L}})$
	2	1	$\mathscr{K}_{\mathscr{J}\mathscr{J}}\ddot{\Phi}_{\mathscr{J}}$	$\mathfrak{M}_{\mathscr{J}JL}(\ddot{X}_J\dot{X}_L+2\dot{X}_J\dot{X}_L)$	$\mathfrak{M}_{\mathscr{L}IJ}(\ddot{X}_J\dot{H}_{\mathscr{L}}+2\dot{X}_J\ddot{H}_{\mathscr{L}}$ $+2\ddot{X}_J\dot{H}_{\mathscr{L}}+\dot{X}_J\ddot{H}_{\mathscr{L}})$
	1	2	$2\mathscr{K}_{\mathscr{J}\mathscr{J}}\ddot{\Phi}_{\mathscr{J}}$	$\mathfrak{M}_{\mathscr{J}JL}(\ddot{X}_J\dot{X}_L+2\dot{X}_J\dot{X}_L)$	$\mathfrak{M}_{\mathscr{L}IJ}(\ddot{X}_J\dot{H}_{\mathscr{L}}+2\dot{X}_J\dot{H}_{\mathscr{L}}$ $+2\dot{X}_J\ddot{H}_{\mathscr{L}}+\dot{X}_J\ddot{H}_{\mathscr{L}})$
	0	3	$3\mathscr{K}_{\mathscr{J}\mathscr{J}}\ddot{\Phi}_{\mathscr{J}}$	$3\mathfrak{M}_{\mathscr{J}JL}\ddot{X}_J\dot{X}_L$	$3\mathfrak{M}_{\mathscr{L}IJ}(\ddot{X}_J\dot{H}_{\mathscr{L}}+\dot{X}_J\ddot{H}_{\mathscr{L}})$
4	4	0	0	$\mathfrak{M}_{\mathscr{J}JL}(4\dddot{X}_J\dot{X}_L+3\ddot{X}_J\ddot{X}_L)$	$\mathfrak{M}_{\mathscr{L}IJ}(4\dddot{X}_J\dot{H}_{\mathscr{L}}+6\ddot{X}_J\ddot{H}_{\mathscr{L}}$ $+4\dot{X}_J\dddot{H}_{\mathscr{L}})$
	3	1	$\mathscr{K}_{\mathscr{J}\mathscr{J}}\dddot{\Phi}_{\mathscr{J}}$	$\mathfrak{M}_{\mathscr{J}JL}(\dddot{X}_J\dot{X}_L+3\ddot{X}_J\dot{X}_L$ $+3\ddot{X}_J\ddot{X}_L)$	$\mathfrak{M}_{\mathscr{L}IJ}(\dddot{X}_J\dot{H}_{\mathscr{L}}+3\ddot{X}_J\ddot{H}_{\mathscr{L}}$ $+3\ddot{X}_J\dot{H}_{\mathscr{L}}+3\dot{X}_J\ddot{H}_{\mathscr{L}}$ $+3\dot{X}_J\dddot{H}_{\mathscr{L}}+\ddot{X}_J\ddot{H}_{\mathscr{L}})$
	2	2	$2\mathscr{K}_{\mathscr{J}\mathscr{J}}\dddot{\Phi}_{\mathscr{J}}$	$\mathfrak{M}_{\mathscr{J}JL}(2\dddot{X}_J\dot{X}_L+2\ddot{X}_J\dot{X}_L$ $+\ddot{X}_J\ddot{X}_L+2\dot{X}_J\dddot{X}_L)$	$\mathfrak{M}_{\mathscr{L}IJ}(2\dddot{X}_J\dot{H}_{\mathscr{L}}+2\ddot{X}_J\dot{H}_{\mathscr{L}}$ $+\ddot{X}_J\ddot{H}_{\mathscr{L}}+4\dddot{X}_J\dddot{H}_{\mathscr{L}}$ $+\ddot{X}_J\dddot{H}_{\mathscr{L}}+2\dddot{X}_J\ddot{H}_{\mathscr{L}}$ $+2\dot{X}_J\dddot{H}_{\mathscr{L}})$
	1	3	$3\mathscr{K}_{\mathscr{J}\mathscr{J}}\dddot{\Phi}_{\mathscr{J}}$	$\mathfrak{M}_{\mathscr{J}JL}(3\dddot{X}_J\dot{X}_L+\ddot{X}_J\dot{X}_L$ $+3\dddot{X}_J\ddot{X}_L)$	$\mathfrak{M}_{\mathscr{L}IJ}(3\dddot{X}_J\dot{H}_{\mathscr{L}}+\ddot{X}_J\dot{H}_{\mathscr{L}}$ $+3\dddot{X}_J\ddot{H}_{\mathscr{L}}+3\ddot{X}_J\dddot{H}_{\mathscr{L}}$ $+\dot{X}_J\ddot{H}_{\mathscr{L}}+3\dddot{X}_J\dddot{H}_{\mathscr{L}})$
	0	4	$4\mathscr{K}_{\mathscr{J}\mathscr{J}}\ddot{\Phi}_{\mathscr{J}}$	$\mathfrak{M}_{\mathscr{J}JL}(4\ddot{X}_J\dot{X}_L$ $+3\ddot{X}_J\ddot{X}_L)$	$\mathfrak{M}_{\mathscr{L}IJ}(4\ddot{X}_J\dot{H}_{\mathscr{L}}+6\ddot{X}_J\ddot{H}_{\mathscr{L}})$ $+4\dot{X}_J\ddot{H}_{\mathscr{L}})$

global approximation vectors. Hence, this matrix is factored only once regardless of the number of global approximation vectors generated. If the global approximation vectors are generated at $\lambda = q = 0$, then $\Phi_{\mathscr{J}} = 0$, $H_{\mathscr{J}} = 0$, and $X_J = 0$. Also, all the derivatives $\partial^n/\partial\lambda^n\,\Phi_{\mathscr{J}}$, $\partial^n/\partial\lambda^n\,H_{\mathscr{J}}$, and $\partial^n/\partial\lambda^n\,X_J$ vanish and Eqs. (B1) are thus simplified. The computational effort in evaluating the global approximation vectors is thereby reduced.

References

[1] Whitney, J.M., "Analysis of Anisotropic Rectangular Plates," *AIAA Journal*, Vol. 10, 1972, pp. 1344-1345.

[2] Sun, C.T., "Double Fourier Series Solution to General Anisotropic Plates," *Journal of Mathematics and Physical Science*, Vol. 6, 1972, pp. 205-223.

[3] Chia, C.Y., *Nonlinear Analysis of Plates*, McGraw-Hill Book Co., New York, 1980.

[4] Noor, A.K. and Camin, R.A., "Symmetry Considerations for Anisotropic Shells," *Computer Methods in Applied Mechanics and Engineering*, Vol. 9, 1976, pp. 317-335.

[5] Noor, A.K., Mathers, M.D., and Anderson, M.S., "Exploiting Symmetries for Efficient Postbuckling Analysis of Composite Plates," *AIAA Journal*, Vol. 15, 1977, pp. 24-32.

[6] Noor, A.K. and Peters, J.M., "Model-Size Reduction Technique for the Analysis of Symmetric Anisotropic Structures," *Engineering Computations*, Vol. 2, No. 4, Dec. 1985, pp. 885-892.

[7] Noor, A.K., "Reduction Method for the Nonlinear Analysis of Symmetric Anisotropic Panels," *Finite Element Methods for Nonlinear Problems*, edited by P.G. Bergan, K.J. Bathe, and W. Wunderlich, Springer-Verlag, 1986, pp. 389-407.

[8] Noor, A.K. and Peters, J.M., "Mixed Models and Reduced/Selective Integration Displacement Models for Vibration Analysis of Shells," *Hybrid and Mixed Finite Element Models*, John Wiley & Sons, New York, 1983, Chap. 28, pp. 537-564.

[9] Noor, A.K. and Andersen, C.M., "Mixed Models and Reduced/Selective Integration Displacement Models for Nonlinear Shell Analysis," *International Journal for Numerical Methods in Engineering*, Vol. 18, 1982, pp. 1429-1454.